Midinfrared unipolar photoluminescence in InAs/GaAs self-assembled quantum dots

S. Sauvage, P. Boucaud,* and T. Brunhes
Institut d'Électronique Fondamentale, UMR CNRS 8622, Bât. 220, Université Paris-Sud, 91405 Orsay, France

A. Lemaître and J.-M. Gérard
France Telecom, CNET Bagneux, 196 Av. H. Ravera, 92225 Bagneux, France

(Received 19 January 1999; revised manuscript received 19 July 1999)

We have investigated the midinfrared unipolar photoluminescence in InAs/GaAs self-assembled quantum dots. Resonant emissions between confined levels are clearly observed at low temperature at around 10 μm wavelength. The unipolar emissions are polarized either in the layer plane or along the z growth axis of the quantum dots. The emissions are associated with hole transitions that involve the ground and the excited hole states. The quenching due to Pauli blocking of the unipolar emission lines involving the hole ground state is observed when this state is completely filled. An intradot nonradiative lifetime $\tau \approx 25$ ps is deduced for the different levels from the midinfrared emitted power. [S0163-1829(99)14947-6]

Semiconductor quantum dots are heterostructures with a confinement potential in the three space directions. This three-dimensional (3D) confinement potential leads to distinctive features with some similarity with those observed in atomic physics. The semiconductor quantum dots are often referred to as ''artificial atoms.'' One of the most striking features is the δ-like density of states for the quantum dots, which leads to well-defined excited levels in the conduction and valence band. The excited levels in self-assembled quantum dots have been observed by several techniques, including photoluminescence at high pump intensities,[1,2] the study of the interband absorption spectrum,[3] capacitance measurements,[4] and more recently by intersublevel (or intraband) absorption.[5–7] The experimental study of the energy diagram and the density of states of self-assembled quantum dots remains nowadays a subject of intense research and represents a very important issue for a comprehensive understanding of the quantum-dot properties.

Apart from the spectroscopy, the study of self-assembled quantum dots is still attracting a lot of interest due to the predicted slowing of the intradot carrier relaxation.[8] This slowing, which is often called the ''phonon bottleneck'' in the literature, is directly associated with the δ-like density of states and the difficulty to conserve the energy by inelastic phonon scattering. The intradot carrier relaxation has been investigated by several different techniques including time-resolved photoluminescence[9–11] and saturation of both interband[12] and intraband absorptions.[13] All these experiments have shown that the intradot carrier relaxation is effectively slowed down in quantum dots as compared to the carrier relaxation in quantum wells. The relaxation times that are experimentally found of the order of a few picoseconds or a few tens of picoseconds are nonetheless not as long as those initially predicted.[8] This feature can be mainly explained by the role of multiphonon relaxation[14] or Auger-assisted recombinations.[15] We emphasize that the experimental relaxation times reported in the literature are still dispersed by at least an order of magnitude. The analysis of the intradot carrier relaxation remains therefore an important issue.

In this paper, we report on the unipolar emission in InAs/GaAs self-assembled quantum dots. We show that the study of midinfrared unipolar photoluminescence can provide valuable information on the quantum dots. This technique can simultaneously probe the excited levels of the quantum dots and give access to the intradot carrier relaxation time. We have experimentally observed unipolar emissions involving different hole states of the quantum dots. The intradot nonradiative lifetime from the different excited levels is deduced from the midinfrared emitted power. We show that the infrared spontaneous emission, associated with the h_{000} hole ground state, is quenched due to the Pauli exclusion principle when the ground state of the quantum dots is completely filled.

The InAs/GaAs self-assembled quantum dots investigated in this work were grown by molecular beam epitaxy. The growth of the quantum dots is performed at 520 °C under As_4 beam pressure.[6] The quantum-dot layers, which are grown on a heavily doped (2×10^{18} cm^{-3}) GaAs substrate, are nominally undoped. The active region of the sample consists of 20 InAs quantum-dot layers separated by 50-nm-thick GaAs barriers. The active region is embedded in a midinfrared waveguide, which consists of an $Al_{0.9}Ga_{0.1}As$ 5-μm-thick cladding layer followed by a 2-μm-thick GaAs layer, the active region, and a 2.5-μm GaAs top layer. Cross-section transmission electronic microscopy images of quantum-dot samples grown in similar conditions show that the quantum dots have a lens-shape geometry with an average dot base diameter $\approx$25 nm and a height $\approx$25 nm. The areal dot density is estimated around 4×10^{10} cm^{-2}.

The midinfrared photoluminescence experiments have been performed at low temperature using the emission port of a Fourier-transform infrared spectrometer. The quantum dots are optically pumped with a Ti:sapphire laser. The interband optical pumping is mechanically chopped at 3 kHz. The Fourier transform infrared spectrometer is operated in step-scan mode at a very low frequency (one mirror step every 25 s). The collected midinfrared signal recorded by a mercury-cadmium-telluride photodetector is filtered by a lock-in amplifier before Fourier transform. This experimental

setup is very sensitive and allows the measurement of signals as low as hundreds of picowatts in the midinfrared after a few hours of collection. A long-wavepass interference filter (6.7 μm cutoff wavelength) is set in front of the detector in order to reject the interband photoluminescence.

The photoinduced absorption spectrum of the quantum-dot sample has been measured at room temperature. To perform this experiment, midinfrared light has been injected through the cleaved facet of the waveguide with an infrared microscope coupled to the Fourier-transform infrared spectrometer. The quantum-dot photoinduced absorption is measured as the normalized variation of transmission of the infrared light in the presence of or without interband optical pumping.[6] The interband pump wavelength is set at 848 nm. Although the pump energy is larger than the GaAs band gap at room temperature, the quantum-dot layers that lie 2.5 μm below the surface are sufficiently populated to observe the photoinduced absorption of the quantum dots. The photoinduced absorption spectrum is dominated by two resonances, as previously reported in Ref. 6. The first resonance is maximum at an energy of 105 meV with a 20-meV full width at half maximum, whereas the second resonance is maximum at around 195 meV with a much larger broadening ($\approx$80 meV). The assignment of the intraband transitions is made on the basis of the absorption spectra reported in *n*- and *p*-doped samples.[7,16] The low-energy (105-meV) resonance is attributed to the h_{000}-h_{001} hole intersublevel transition, while the high-energy (195-meV) transition corresponds to an e_{000}-continuum electronic intersublevel absorption.

At low excitation density and low temperature, the interband photoluminescence spectrum exhibits a maximum at 1.17 eV. The interband spontaneous emission, which corresponds to the quantum-dot ground-state excitonic recombination, is inhomogeneously broadened by the dot size distribution (40 meV full width at half maximum). As the pump intensity increased, the photoluminescence associated with the first excited states (e_{100},h_{100}) can be observed. However, the interband and intraband recombinations are not governed by the same dipolar matrix elements. Since the intraband photoluminescence starting from the e_{100} and h_{100} energy states is beyond the detector cutoff energy, the comparison between interband and intraband photoluminescence spectra is not straightforward and does not bring valuable information.

The midinfrared photoluminescence spectrum of the quantum dots is presented for the two TM and TE polarizations in Fig. 1. The TM polarization corresponds to an electric field direction along the growth axis of the quantum dots. The TE polarization corresponds to an electric field direction in the layer plane. The sample temperature is set at 20 K. The sample is optically pumped by the surface, and the emission is collected by the cleaved facet. The interband optical pumping is set at 848 nm and allows to directly generate carriers in the wetting layer. In this experimental configuration, and even if the sample is set on the emission port of the spectrometer, a weak absorption is observed. This residual absorption is associated with the room-temperature blackbody background modulation, which is due to the carriers injected in the structure.[17] The spectra in Fig. 1 have been corrected from this weak absorption. Three resonant emissions at different energy maxima are clearly observed for

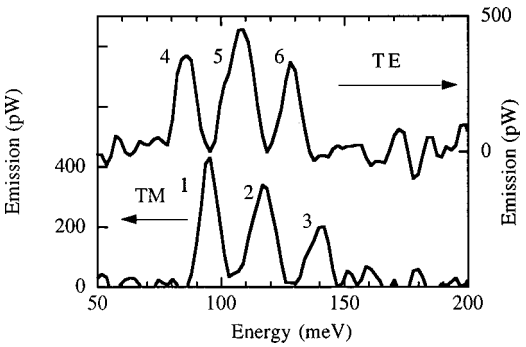

FIG. 1. Midinfrared unipolar photoluminescence observed in TM (bottom curve, left scale) and TE polarization (top curve, right scale). The temperature is 20 K. The interband pump intensity is 70 W cm^{-2} at 848 nm.

both polarizations. The broadening (full width at half maximum) of the transitions varies from 9 to 15 meV. It is important to emphasize that the analysis of the emission spectra requires the emission dependence versus the polarization. Without polarizers, only a broad emission band with no well-defined peaks is observed.

The resonances reported in Fig. 1 exhibit a nearly regular energy separation. As will be shown below, we attribute this peculiar spectral shape to the electronic structure of the quantum dots. We have performed similar experiments in quantum wells (Ref. 17 and references therein) as well as in doped quantum dots. In both cases, the active region was embedded in a waveguide structure. In quantum-well samples, the emission was, as expected, TM-polarized and resonant at the predicted intersubband transition energy. In doped quantum dots, we did not observe such a clear signature of the intraband emission. This feature is partly attributed to a modification of the relaxation mechanisms as well as to a lower efficiency of the pumping mechanism in doped samples. The emission spectra reported in Fig. 1 are therefore specific of the intraband emission in self-assembled quantum dots.

The midinfrared collected power remains very weak, less than 1 nW in the present experimental conditions. This feature is a direct consequence of the efficient nonradiative intradot relaxation time (a few or tens of picoseconds) as compared to the long radiative lifetime (a few microseconds) for the intraband transitions. Such a situation is identical to that observed for the unipolar intersubband emission in quantum wells.[17] Note that the weak quantum efficiency of the spontaneous unipolar emission did not prevent observation of the laser emission in an optimized quantum-well structure.[18]

The dependences of the midinfrared optical power of the 95- and 115-meV emission lines are reported in Fig. 2 as a function of the interband pump intensity. These emission lines correspond to TM polarization. Two distinct behaviors are observed. In both cases, the infrared emitted power first increases with the pump intensity since the intersublevel emission is proportional to the number of photoinjected carriers at low pump intensity. However, the quenching of the midinfrared luminescence is different for the two emission lines. The 95-meV emission vanishes above 300 W cm^{-2}, while the 115-meV emission line can still be observed at this intensity. Note that the error bars in Fig. 2 reflect the precision that we can achieve between successive measurements.

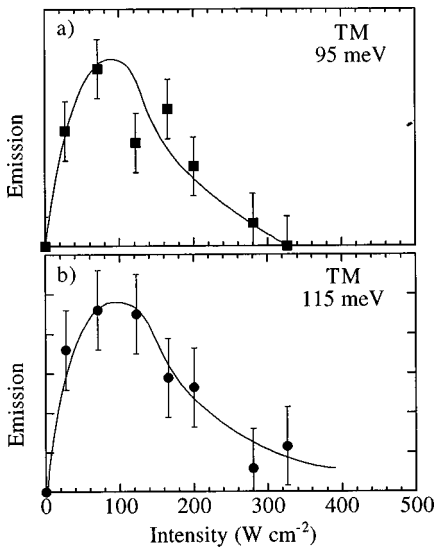

FIG. 2. Amplitude of the 95-meV (squares) and 115-meV (dots) emission lines as a function of the interband pump intensity. The full lines are guides to the eye.

In particular, they account for variations in the coupling efficiency and in the background signal. For a given polarization, the amplitude of each emission peak is measured on the same spectrum. There is therefore a significant difference between the data points reported at high intensities in Figs. 2(a) and 2(b).

The same analysis has been undertaken for all the unipolar emission lines. In TM polarization, the 140-meV emission also vanishes beyond 300 $\mathrm{W\,cm^{-2}}$. In TE polarization, only the 130-meV emission is quenched for intensities higher than 300 $\mathrm{W\,cm^{-2}}$. The two other emission lines exhibit a pump intensity dependence similar to the one reported for the 115-meV emission. It is worth noticing that an intensity of 100 $\mathrm{W\,cm^{-2}}$, which corresponds to the onset of the photoluminescence quenching, also corresponds to the intensity where the dot ground state starts to be completely filled, as observed by photoinduced absorption measurements.[6] The quenching of the unipolar emission is therefore attributed to the Pauli exclusion principle, which forbids the spontaneous emission when the dot ground state is filled. It indicates that the emission lines that disappear first involve the ground state of the quantum dots. Note that a similar quenching due to the Pauli principle has recently been reported in interband absorption measurements.[3] In these experiments, the interband absorption is progressively quenched as electrons are loaded in the quantum dots. When the dot ground state is fully occupied, the interband absorption involving the electron ground state vanishes.

The assignment of the optical transitions experimentally observed are made on the basis of the infrared absorption and emission spectra of the self-assembled quantum dots along with numerical simulations. Previous studies on the intraband absorption in self-assembled quantum dots have been reported in Refs. 6, 7, 13, 16, and 19. The confined energy levels in the lens-shaped quantum dots have been calculated by solving numerically the three-dimensional (3D) Schrödinger equation in the effective-mass approximation.[19] The electronic (hole) confined levels are denoted $e_{n_x,n_y,n_z}(h)$. The subscripts n_x, n_y, n_z are given by reference to a parallelelipedal quantum dot with infinite potential barriers, where they correspond to the number of nodes of the envelope wave functions along the x, y, and z directions, respectively. Note that the calculation of the confined energy states in quantum dots remains a difficult issue. The exact value of the confinement energies is strongly dependent on the quantum-dot size, shape, geometry, strain relaxation, and composition. These parameters are expected to vary within each layer and from layer to layer in stacked quantum-dot samples, thus limiting the accuracy of any type of calculation unless these parameters are fully taken into account. The single-band effective-mass model that we have used does not predict the exact energy values of the confined states. However, up to now, this model, which accounts for the three-dimensional geometry of the quantum dots, has provided a good basis for the interpretation of the intraband absorption spectra and particularly the associated polarization selection rules and the dipole matrix elements.

In the conduction band and for the present quantum-dot size distribution, only three levels (e_{000} and the doubly degenerate e_{100} states) are bound. The e_{110} state is very weakly bound and hybridized with the wetting layer continuum states. The photoinduced absorption spectrum of the sample shows that the e_{000}-continuum transition is maximum around 200 meV. The energy of the e_{000}-e_{100} intraband transition is, on the other hand, predicted to occur below the detector cutoff energy (80 meV). The unipolar emission spectra reported in Fig. 1 are therefore associated with the hole intraband transitions. In absorption, the main transition observed in TM polarization corresponds to the h_{000}-h_{001} transition. For the present sample, this transition is maximum at room temperature at 105 meV. We attribute the dominant emission at 95 meV observed in TM polarization to this h_{000}-h_{001} transition. This assumption is in agreement with the quenching observed for this transition at high interband pump intensity. At this step, the assignment of the other transitions is straightforward since it only requires one to take into account the allowed transitions predicted by the numerical calculations.

A key feature is related to the polarization selection rules for intersublevel transitions, which is predicted by the numerical modeling. This polarization dependence is particularly relevant for the assignment of the different observed transitions. The origin of the different transitions reported in Fig. 1 is summarized in Fig. 3. We postulate that the transitions that are not completely quenched at 300 $\mathrm{W\,cm^{-2}}$ involve the excited hole states. Note that the energy structure involving the six transitions is very consistent. By energy differences, we can deduce experimental transition energies for h_{100}-h_{000} to be 33 meV and for h_{110}-h_{100} to be 30 meV. For clarity, only the intersublevel transitions experimentally observed in the 90–185-meV energy spectral range are reported in Fig. 3. Other transitions, like the in-plane polarized h_{100}-h_{000} transition, should be observable. However, the energy of such a transition is below the detector cutoff energy. In the absence of saturation, the infrared emitted power can be calculated according to[17]

$$P = \frac{e^2\omega^4 d^2 \tau \alpha_{\mathrm{ib}} P_{\mathrm{ib}}}{3\pi c^3 \epsilon_0 h \nu_{\mathrm{ib}}} \frac{4n^2}{(n+1)^2} \eta_{\mathrm{coll}}, \qquad (1)$$

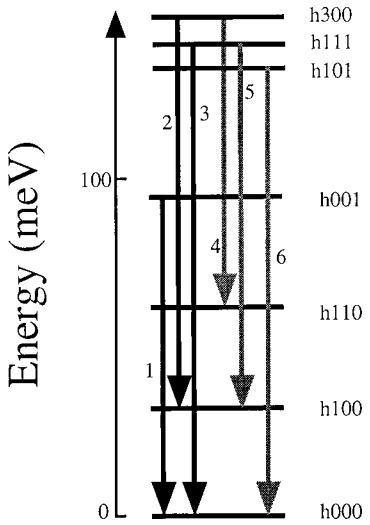

FIG. 3. Schematic diagram showing the hole confined states associated with unipolar emission. The lines labeled 1, 2, and 3 correspond to the 95-, 115-, and 140-meV emission lines observed in TM polarization. They are attributed to the h_{000}-h_{001}, h_{100}-h_{300}, and h_{000}-h_{111} transitions, respectively. These transitions are characterized by theoretical dipole matrix elements of 0.36, 0.31, and 0.11 nm. The lines labeled 4, 5, and 6 correspond to the 85-, 107-, and 127-meV emission lines observed in TE polarization. They are attributed to the h_{110}-h_{300}, h_{100}-h_{111}, and h_{000}-h_{101} transitions, respectively. Only the levels involved in the unipolar emission appear on the graph. The origin of the energy scale is taken at the hole ground state.

where n is the refractive index of the material, $h\nu_{ib}$ the interband energy, ω the pulsation of the emitted signal, d the intersublevel dipole length ($d \approx 0.35$ nm for the h_{000}-h_{001} transition), τ the intradot nonradiative hole relaxation time from the upper level, α_{ib} the fraction of interband power absorbed by the quantum dots, P_{ib} the interband optical power, and η_{coll} the collection efficiency of the luminescence that is coupled out of the sample (6×10^{-3}). e is the electronic charge, c the speed of light, and ϵ_0 the vacuum permittivity. The coefficient α_{ib} can be either estimated from the interband absorption coefficient or deduced from the pump power dependence of the emission. For a 200-W cm^{-2} pump intensity, the amplitude of the h_{000}-h_{001} emission is divided by a factor of 2. This quenching corresponds approximately to an equivalent hole density of 1.5 carriers per dot, i.e., 6×10^{10} carriers per square centimeter. This leads to an α_{ib} coefficient equal to 0.9 for the 20-dot layer planes.

Starting from the 430 pW midinfrared emitted power for the h_{000}-h_{001} transition for an interband pump power of 500 mW at 848 nm, an intradot nonradiative lifetime of 25 ps is deduced for the h_{001} level. It is worth noticing that this value is dependent on the exact emitted power coupled out of the waveguide. Assuming that all the levels are equally populated, the relative amplitudes of the unipolar emission lines depend on the relative values of the energies, dipole matrix elements, and intradot relaxation times. Starting from the values of the dipole matrix elements given by the numerical calculations, one finds an intradot lifetime $\tau \approx 12.5$ and 27 ps for the h_{300} and h_{111} level, respectively. The intradot lifetimes involving separate levels are therefore of the same order of magnitude.

We emphasize that the lifetime values deduced from unipolar measurements depend on the exact midinfrared optical power coupled out of the waveguide and on the exact values of dipole matrix elements. Note that a variation of the quantum-dot geometry can lead to consequent variations on the dipole matrix elements. A more accurate description should also take into account all the relaxation mechanisms and pathways inside the quantum dots, which is beyond the scope of this paper. These lifetimes are nonetheless of the same order of magnitude as the relaxation times reported by time-resolved photoluminescence experiments.[9,11] It is not surprising since, although the unipolar emission differs from the bipolar interband emission, the experimental conditions are similar to those of photoluminescence, i.e., involving the presence of both photoinduced electron and holes. It is worth noticing that the unipolar emission is observed in the present experimental conditions for a relatively high injected carrier density. Auger-related relaxation mechanisms are likely to occur in these conditions[15] and modify the relaxation time as a function of the interband pump intensity.

In conclusion, we have shown that midinfrared unipolar photoluminescence is a sound technique to investigate different excited states simultaneously in self-assembled quantum dots and to measure the intradot lifetime. The observation of unipolar spontaneous emission in quantum dots constitute a first step towards the realization of midinfrared unipolar lasers, like the quantum cascade lasers developed with semiconductor quantum wells.[18]

This work was supported by DGA under Contract No. 97062/DPS.

*Electronic address: phill@ief.u-psud.fr

[1] M. Grundmann *et al.*, Appl. Phys. Lett. **68**, 979 (1996).
[2] K. H. Schmidt *et al.*, Phys. Rev. B **54**, 11 346 (1996).
[3] R. J. Warburton *et al.*, Phys. Rev. Lett. **79**, 5282 (1997).
[4] H. Drexler *et al.*, Phys. Rev. Lett. **73**, 2252 (1994).
[5] M. Fricke *et al.*, Europhys. Lett. **36**, 197 (1996).
[6] S. Sauvage *et al.*, J. Appl. Phys. **82**, 3396 (1997).
[7] S. Sauvage *et al.*, Appl. Phys. Lett. **71**, 2785 (1997).
[8] H. Benisty *et al.*, Phys. Rev. B **44**, 10 945 (1991).
[9] J.-M. Gérard, in *Confined Electrons and Photons*, edited by E. Burstein and C. Weisbuch (Plenum, New York, 1995).
[10] B. Ohnesorge *et al.*, Phys. Rev. B **54**, 11 532 (1996).
[11] R. Heitz *et al.*, Phys. Rev. B **56**, 10 435 (1997).
[12] T. S. Sosnowski *et al.*, Phys. Rev. B **57**, R9423 (1998).
[13] S. Sauvage *et al.*, Appl. Phys. Lett. **73**, 3818 (1998).
[14] T. Inoshita and H. Sakaki, Phys. Rev. B **46**, 7260 (1992).
[15] U. Bockelmann and T. Egeler, Phys. Rev. B **46**, 15 574 (1992).
[16] S. Sauvage *et al.*, Phys. Rev. B **59**, 9830 (1999).
[17] S. Sauvage *et al.*, Appl. Phys. Lett. **71**, 1183 (1997).
[18] J. Faist *et al.*, Science **264**, 553 (1994).
[19] S. Sauvage *et al.*, Phys. Rev. B **58**, 10 562 (1998).